TIME DOMAIN AND FREQUENCY DOMAIN IMPLEMENTATIONS OF FMT MODULATION ARCHITECTURES

Andrea M. Tonello

Università di Udine - Dipartimento di Ingegneria Elettrica Gestionale e Meccanica (DIEGM)
Via delle Scienze 208 - 33100 Udine - Italy
phone: +39 0432 558042 - fax: +39 0432 558251 - e-mail: tonello@uniud.it

ABSTRACT

This paper deals with the design and implementation of a Filtered Multitone (FMT) modulation system. FMT generalizes the popular OFDM scheme through the deployment of sub-channel shaping filters. We address the implementation problem and we describe (and compare in terms of complexity) two efficient implementation methods in the time domain (TD) and another one in the frequency domain (FD). We consider the design of the prototype pulse and we propose to synthesize it in the FD with a small number of frequency components. This allows to efficiently implement the FMT scheme through the FD architecture. A simple FD equalization scheme is also proposed and its performance is evaluated in typical wireless fading channels. The results show that FMT performs better than OFDM with and without channel coding.

1. INTRODUCTION

In this paper we consider design and implementation aspects of multicarrier modulation based architectures [1]. The main idea behind these architectures is to convert a sequence of data symbols at high rate, into a number of sub-sequences at low rate. Each low rate sequence is transmitted through a sub-channel that is shaped with an appropriate filter centered on a given sub-carrier. In particular, we consider Filtered Multitone (FMT) modulation [2] that is a discrete time implementation of a multicarrier system where sub-carriers are uniformly spaced and the sub-channel pulses are identical (Fig. 1). Discrete Multitone Modulation (DMT) (also referred to as orthogonal frequency division multiplexing (OFDM)) can be viewed as an FMT scheme that deploys rectangular time domain filters. FMT modulation can be deployed for transmission over broadband frequency selective channels both in wireline [2] and in wireless scenarios [3]-[5]. The channel frequency selectivity introduces intercarrier (ICI) and intersymbol (ISI) interference at the receiver. The design of the sub-channel filters, and the choice of the sub-carrier spacing in an FMT system, aims at subdividing the spectrum in a number of sub-channels that do not overlap in the frequency domain, such that we can avoid the ICI and get low ISI contributions. In a DMT system the insertion of a cyclic prefix longer than the channel time dispersion is such that the ISI and ICI are eliminated, and the receiver simplifies to a simple one-tap equalizer per sub-channel. The key aspects of FMT modulation are the design of the prototype pulse, the efficient implementation of the synthesis/analysis filter banks, and finally the design of the multi-channel detector (equalizer). In this paper we focus on the efficient implementation. We review the implementation proposed by Cherubini *et al*. [2] that is obtained by the polyphase decomposition of the signals. Then, we propose other two implementations one of which is in the time domain (TD) and another in the frequency domain (FD). We propose a FD design of the prototype pulse. Finally, we describe a simple FD equalizer and we report a performance comparison with OFDM over typical wireless fading channels.

2. FMT MODULATION SCHEME

An FMT modulation based architecture is depicted in Fig. 1 where we assume the following system parameters: T is the transmission period; $W = 1/T$ is the transmission bandwidth; M is the number of sub-channels; $T_0 = NT$ is the sub-channel symbol period; f_k is the k-th sub-carrier; $g(nT)$ is the prototype pulse; $R = M/T_0$ is the overall transmission rate in symbol/s. The transmitter (synthesis stage) generates the signal

$$x(iT) = \sum_{k=0}^{M-1} \sum_{l \in \mathbb{Z}} a^{(k)}(lT_0) g(iT - lT_0) e^{j2\pi f_k iT} \qquad i \in \mathbb{Z} \qquad (1)$$

where $a^k(lT_0)$ is the sequence of complex data symbols, e.g., M-QAM, that is transmitted on sub-channel $k = 0,...,M-1$ at rate $1/T_0$. If the sub-carrier spacing $f_k - f_{k-1}$ is larger than $1/T_0$ the scheme is referred to as non-critically sampled FMT, otherwise if $f_k - f_{k-1} = 1/T_0$ it is referred to as critically sampled FMT [2]. The implementation of the modulator according to (1) is inefficient. Assuming that the prototype pulse is FIR with L_g coefficients, it requires a number of complex operations (sums and multiplications) per output coefficient $x(iT)$ equal to $2M\lfloor L_g / N \rfloor + M - 1$. The signal (1) is digital-to-analog converted and transmitted over the communication channel (after RF conversion, in wireless applications). The received lowpass signal is analog-to-digital converted to obtain $y(iT)$ and then it is passed through an analysis filter bank with prototype pulse $h(nT)$. The sampled outputs at rate $1/T_0$ are

$$z^{(k)}(lT_0) = \sum_{i \in \mathbb{Z}} y(iT) e^{-j2\pi f_k iT} h(lT_0 - iT) \qquad k = 0,...,M-1 \qquad (2)$$

If the analysis pulse is FIR with L_h coefficients, (2) requires $2ML_h/T_0$ operations per second.

In the following sub-sections we describe three possible efficient implementations two of which are in the TD and one in the FD.

3. BASELINE IMPLEMENTATION: *METHOD A*

Let us assume the sub-carriers to be $f_k = k/(MT)$. Then, following [2], if we compute the polyphase decomposition of (1) with period $T_1 = MT \le T_0$ we obtain

$$\begin{aligned} x^{(i)}(mT_1) &= x(iT + mT_1) \quad i = 0,...,M-1,\ m \in \mathbb{Z} \\ &= \sum_{l\in\mathbb{Z}} \sum_{k=0}^{M-1} a^{(k)}(lT_0) e^{j\frac{2\pi}{M}ik} g(iT + mT_1 - lT_0). \end{aligned} \tag{3}$$

With the following definitions

$$A^{(i)}(lT_0) = \sum_{k=0}^{M-1} a^{(k)}(lT_0) e^{j\frac{2\pi}{M}ik} \tag{4}$$

$$p = \lfloor mM/N \rfloor \quad q = (mM)\%N \tag{5}$$

$$\begin{aligned} g(iT + mT_1 - lT_0) &= g^{(i)}(mT_1 - lT_0) = g^{(i)}(pT_0 - lT_0 + qT) \\ &= g^{(i)}(pT_0 - lT_0; mT_1) \end{aligned} \tag{6}$$

where $\lfloor . \rfloor$ and % are the floor and remainder functions, we obtain

$$x^{(i)}(mT_1) = \sum_{l\in\mathbb{Z}} A^{(i)}(lT_0) g^{(i)}(pT_0 - lT_0; mT_1). \tag{7}$$

Therefore, the FMT signal (Fig. 2) can be synthesized via an M-point inverse discrete Fourier transform (IDFT), followed by time-variant filtering at rate $1/T_0$ with the pulses $g^{(i)}(lT_0; mT_1)$, and finally P/S conversion. Note that the polyphase components of the prototype pulse are cyclically time-variant if $T_0 > T_1$ with period $l.c.m.(T_1, T_0)$.

This implementation has been proposed in [2]. Assuming to implement the IDFT with an inverse fast Fourier transform (FFT), the scheme requires $(\alpha M Log_2 M + 2N\lfloor L_g/N \rfloor - 1)/T_0$ operations per second where $\alpha \ge 2$ is a constant related to the FFT algorithm.

The analysis filterbank (2) can be implemented as follows

$$\begin{aligned} z^{(k)}(lT_0) &= \sum_{m\in\mathbb{Z}} \sum_{i=0}^{M-1} y^{(i)}(mT_1) e^{-j\frac{2\pi}{M}ik} h(lT_0 - mT_1 - iT) \\ &= \sum_{i=0}^{M-1} Z^{(i)}(lT_0) e^{-j\frac{2\pi}{M}ik} \end{aligned} \tag{8}$$

where

$$Z^{(i)}(lT_0) = \sum_{m\in\mathbb{Z}} y^{(i)}(mT_1) h^{(-i)}(pT_1 - mT_1; lT_0) \tag{9}$$

$$h(lT_0 - mT_1 - iT) = h^{(-i)}(pT_1 - mT_1; lT_0) \tag{10}$$

$$p = \lfloor lN/M \rfloor \quad q = (lN)\%M. \tag{11}$$

Therefore, the receiver filter bank (Fig. 2) can be implemented with a S/P conversion of the received signal $y(iT)$, low-rate filtering with the cyclically time-variant pulses $h^{(-i)}(mT_1; lT_0)$, followed by an M-point DFT. The receiver filter bank implementation requires $(\alpha M Log_2 M + M(2\lfloor L_h/M \rfloor - 1))/T_0$ operations per second.

It follows that this implementation of the FMT transmit/receive filter banks is advantageous compared to the direct implementation in (1)-(2), and it is simple if the synthesis and analysis prototype pulses are realized with FIR filters with a small number of coefficients.

4. TD IMPLEMENTATION: *METHOD B*

Herein we propose an alternative way of implementing the synthesis/analysis stages. It is obtained by computing the polyphase decomposition of (1) with period $T_2 = M_2 T$, assuming $M_2 = l.c.m.(M, N) = K_2 M = L_2 N$,

$$\begin{aligned} x^{(i)}(mT_2) &= x(iT + mT_2) \quad i = 0,...,M_2 - 1,\ m \in \mathbb{Z} \\ &= \sum_{l\in\mathbb{Z}} \sum_{k=0}^{M-1} a^{(k)}(lT_0) e^{j\frac{2\pi}{M}ik} g(iT + mT_2 - lT_0) \\ &= \sum_{l\in\mathbb{Z}} A^{(i)}(lT_0) g^{(i)}(mL_2T_0 - lT_0) \end{aligned} \tag{12}$$

where $\{A^{(i)}(lT_0)\}$ are obtained by the M-point IDFT of $\{a^{(k)}(lT_0)\}$ with a cyclic extension of $M_2 - M$ elements. Therefore, the FMT signal (Fig. 3) can be synthesized through an M-point DFT, cyclic extension of the outputs, low-rate filtering with the pulses $g^{(i)}(lT_0) = g(iT + lT_0)$, sampling with period L_2T_0, and P/S conversion. The complexity of this scheme accounts for $(\alpha M Log_2 M + 2N\lfloor L_g/N \rfloor - 1)/T_0$ operations per second (identical to Method A).

Similarly, the analysis filter bank can be implemented as

$$z^{(k)}(lT_0) = \sum_{i=0}^{M_2-1} Z^{(i)}(lT_0) e^{-j\frac{2\pi K_2}{M_2}ik} \tag{13}$$

$$Z^{(i)}(lT_0) = \sum_{m\in\mathbb{Z}} y^{(i)}(mL_2T_0) h^{(-i)}(lT_0 - mL_2T_0). \tag{14}$$

Therefore, the FMT signal (Fig. 3) can be analyzed by low-rate filtering with pulses $h^{(-i)}(lT_0) = h(lT_0 - iT)$, followed by an M_2-point DFT. This filterbank implementation requires $(\alpha M Log_2 M_2 + M_2(2\lfloor L_h/M_2 \rfloor - 1))/T_0$ operations per second that are less than those in Method A if K_2>2.

5. FD IMPLEMENTATION: *METHOD C*

Let us assume the prototype pulse to have duration $T_3 = M_3 T$, with $M_3 = L_3 N$, and let us assume the sub-carriers to be $f_k = (kK_3 + k_0)/M_3$ with $k = 0,...,M-1$ and $M = \lfloor M_3/K_3 \rfloor$. Then, we can write

$$\begin{aligned} x^{(i)}(mT_3) &= x(iT + mT_3) \quad i = 0,...,M_3 - 1,\ m \in \mathbb{Z} \\ &= \sum_{l=-\infty}^{\infty} \sum_{k=0}^{M-1} a^{(k)}(lT_0) g(iT + mT_3 - lT_0) e^{j\frac{2\pi}{M_3}i(kK_3 + k_0)}. \end{aligned} \tag{15}$$

Let us denote with $G^{(n)}$ the DFT with M_3 points of $g(iT)$,

$$G^{(n)} = G(\frac{n}{M_3 T}) = \frac{1}{M_3} \sum_{i=0}^{M_3-1} g(iT) e^{-j\frac{2\pi}{M_3}in}. \tag{16}$$

If for easy of notation we assume $k_0 = 0$, (15) can be manipulated as follows

$$x^{(i)}(mT_3) = \sum_{l=\lfloor i/N \rfloor + mL_3 - L_3 + 1}^{\lfloor i/N \rfloor + mL_3} \sum_{n=0}^{M_3-1} \left(\sum_{k=0}^{M-1} a^{(k)}(lT_0) G^{(n-kK_3)} e^{-j\frac{2\pi}{M_3}((n-kK_3)lN - ni)} \right). \tag{17}$$

Finally,

$$x^{(i)}(mT_3)=\sum_{l=\lfloor i/N\rfloor+mL_3-L_3+1}^{l=\lfloor i/N\rfloor+mL_3}\sum_{n=0}^{M_3-1}B^{(n)}(lT_0)^{j\frac{2\pi}{M_3}ni} \tag{18}$$

$$B^{(n)}(lT_0)=\sum_{k=0}^{M-1}a^{(k)}(lT_0)e^{-j\frac{2\pi}{M_3}(n-kK_3)lN}G^{(n-kK_3)}. \tag{19}$$

This implementation is attractive when the prototype pulse is synthesized in the frequency domain with a small number of non-zero frequency components, i.e., $G^{(n)}\neq 0$ for $n=0,...,K_3-1$. In such a case we can write

$$B^{(n)}(lT_0)=a^{\lfloor n/K_3\rfloor}(lT_0)e^{-j\frac{2\pi}{M_3}(n-\lfloor n/K_3\rfloor K_3)lN}G^{(n\%K_3)}. \tag{20}$$

Therefore, the FMT signal (Fig. 4) can be synthesized by weighting the block of K_3 frequency components of the prototype pulse with each of the M data symbols to obtain (20). Then, we run an M_3-point IDFT, followed by an overlap-and-add operation at rate $1/T_0$ according to (18). The evaluation of the complexity of this implementation yields $(\alpha L_3 Log_2 M_3+3L_3)/T$ operations per second. Although this method may involve a higher number of operations than the Methods A/B, it can be easily and flexibly realized in hardware via an FFT and a overlap-and-add operation.

Now, let us turn the attention to the analysis filter bank (2). Again, with a frequency domain approach we can write

$$\begin{aligned}z^{(k)}(mT_0)&=\sum_i y(mT_0+iT)e^{-j\frac{2\pi K_3}{L_3}km}h(-iT)e^{-j\frac{2\pi K_3}{M_3}ik}\\&=e^{-j\frac{2\pi K_3}{L_3}km}\sum_{n=kK_3}^{kK_3+K_3-1}Y^{(n)}(mT_0)H^{*(n-kK_3)}\end{aligned} \tag{21}$$

where $Y^{(n)}(mT_0)$ and $H^{(n)}$ are the M_3-point DFT of $y(mT_0+iT)$ and $h(iT)$. The equality holds for Parseval theorem under the assumption of a pulse with duration M_3T and K_3 non-zero frequency components. This method (Fig. 4) requires $(\alpha L_3 Log_2 M_3+2L_3)/T$ operations per second.

6. DESIGN OF THE PROTOTYPE PULSE

The design of the prototype pulse is a key issue. To fulfill the orthogonality conditions we look for pulses that are band limited and have Nyquist autocorrelation. A straightforward choice is to use, for instance, a truncated root-raised-cosine pulse. Truncation gives rise to side lobs (thus, to increased ICI) and to non-perfectly raised cosine autocorrelation (thus, to ISI). However, the FIR prototype pulse makes the TD implementation feasible. Vice-versa having in mind the FD implementation, we may want to synthesize the pulse in the FD with a finite number of frequency components. We start by choosing a pulse that belongs to the Nyquist class with roll-off ρ and Nyquist frequency $F_N=1/(2T_0)$. Let $H(f)$ be its frequency response. The K_3 frequency components of the pulse are chosen accordingly to $G(f_n)=\sqrt{H(f_n)}$ where the samples are taken at

$$nF=n\frac{2F_N}{K_3-3}\quad n\in\mathbb{Z},\ |n|\leq\frac{(K_3-1)}{2}. \tag{22}$$

If we use the FD implementation of the FMT scheme with an IDFT of M_3 points, we have that $M_3=N(K_3-3)$, $L_3=(K_3-3)$ since $F=1/(NT)/(K_3-3)=1/(M_3T)$, and $M=\lfloor M_3/K_3\rfloor$. Now, we have some degree of freedom in choosing the function $H(f)$ and the roll-off factor ρ. Herein, we propose a conventional root-raised-cosine spectrum. Furthermore, after fixing K_3, we choose the roll-off as follows

$$\rho=K_3/(K_3-3)-1. \tag{23}$$

With the above design the overall transmission rate equals $R=(K_3-3)/(K_3T)$ $symb/s$ which increases as K_3 increases. In Fig. 5 we plot the impulse response of the prototype pulse for K_3=7, 11, 19 assuming M_3=128. The autocorrelation of the synthesized pulse is only approximately Nyquist. Nevertheless, the signal to ISI power ratio is very high. For instance, with $K_3=11$ the S/I equals 59.76 dB. For comparison, if we used a truncated root-raised-cosine pulse with the same roll-off and duration, we would get an S/I of only 35.76 dB.

7. FD EQUALIZATION IN FREQUENCY SELECTIVE CHANNELS

We herein model the baseband channel with a discrete time filter $g_{CH}(nT)$ that comprises the effect of the DAC and ADC stages. In the wireless context with multipath fading, the channel taps are complex with Gaussian distribution. It follows that the received signal reads

$$y(nT)=\sum_{k=0}^{M-1}\sum_{l=-\infty}^{\infty}a^{(k)}(lT_0)e^{j2\pi f_k lT_0}g_{EQ}^{(k)}(nT-lT_0)+\eta(nT) \tag{24}$$

where the k-th sub-channel equivalent impulse response is

$$g_{EQ}^{(k)}(nT)=\sum_{n=-\infty}^{\infty}g_{CH}(nT-iT)g(iT)e^{j2\pi f_k iT}. \tag{25}$$

Assuming the analysis filterbank to be matched to the equivalent sub-channel responses, i.e., $h^{(k)}(nT)=g_{EQ}^{(k)^*}(-nT)$, the k-th filter output sample reads

$$\begin{aligned}z^{(k)}(mT_0)&=\sum_n y(nT)g_{EQ}^{(k)*}(nT-mT_0)\\&=a^{(k)}(mT_0)\kappa_{EQ}^{(k)}(0)+ISI^{(k)}(mT_0)+ICI^{(k)}(mT_0)+\eta^{(k)}(mT_0)\end{aligned} \tag{26}$$

where the first term represents the useful data contribution, the second additive term is the ISI contribution, the third term is the ICI contribution, and the fourth term is the noise contribution. Further, $\kappa_{EQ}^{(k)}(mT_0)=g_{EQ}^{(k)}*g_{EQ-}^{(k)*}(mT_0)$ is the equivalent sub-channel autocorrelation. If we assume frequency concentrated non-overlapping sub-channels the ICI term is zero. The ISI can be mitigated with some form of equalization, i.e., maximum likelihood sequence estimation, linear or decision feedback equalization [3]-[5]. If the ISI is negligible, we may want to use a simple one tap equalizer. To derive a simple detector we assume that the prototype pulse has short duration, such that convolved with the channel yields an equivalent response with time support approximately equal to M_3T. Then, the matched filtering operation can take place in the frequency domain as in (21) by using $H^{(n)}=G_{EQ}^{(n)*}\approx G^{(n-kK_3)*}G_{CH}^{(n)*}$ where $G^{(n)}$ and $G_{CH}^{(n)}$ are the DFT of the prototype pulse and of the channel. A further simplification can be obtained by choosing, e.g., with a minimum mean-square-error criterion, a single channel weight

$H^{(k)}$ within a single sub-channel k, which corresponds to assume the channel flat within a band K_3F.

8. NUMERICAL RESULTS

In Fig. 6 we show bit-error-rate (BER) performance of the FMT scheme that uses the prototype pulse proposed in Section 6 and the FD equalizer in Section 7. We assume a Rayleigh faded channel with exponential power delay profile (truncated to 32T) with root-mean-square delay spread τ and a 20 MHz bandwidth (as in the WLAN standard IEEE 802.11a). Further, we use BPSK signalling, and parameters M_3=128, K_3=11, M=11. We consider also channel coding with a convolutional encoder of rate ½ and constraint length 5 that is followed by a random bit-interleaver, and a S/P converter to produce M bit streams. The simple FD equalization scheme is deployed under the assumption of knowing the channel. For comparison we report also the BER performance of an OFDM (DMT) system that uses a 128 point FFT, a cyclic prefix of length 32, and data rate identical to the FMT system. The same channel encoder is deployed for the OFDM system. Fig. 6 shows that the BER performance of the FMT system is good even without channel coding. Note also that some frequency diversity exploitation is possible also without coding despite the simple equalization scheme. On the contrary the uncoded OFDM scheme does not provide any diversity gain. With coding there is a deep performance improvement in both the FMT and the OFDM scheme that is more pronounced for high delay spreads as a result of higher frequency diversity. However, the coded FMT scheme shows superior performance than the coded OFDM scheme still having identical data rate and comparable complexity.

9. CONCLUSIONS

We have described and compared in terms of complexity several efficient implementations of an FMT scheme. We have proposed a FD design of the prototype pulse and a simple FD equalization scheme. The performance results show the superiority of the proposed FMT scheme compared to conventional OFDM in wireless fading channels with and without channel coding.

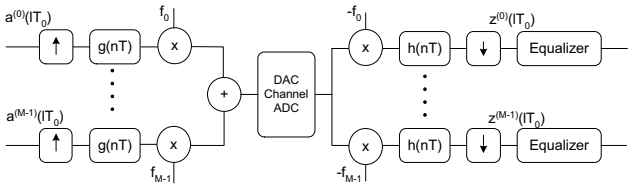

Fig. 1. FMT modulator/demodulator with inefficient implementation.

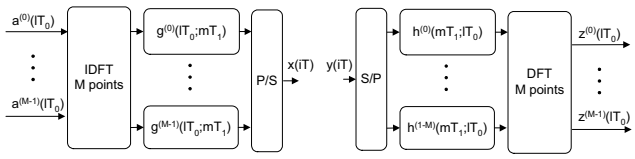

Fig. 2. FMT modulator/demodulator implemented with Method A .

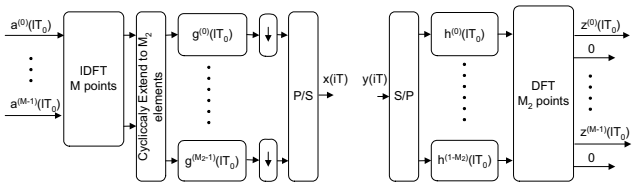

Fig. 3. FMT modulator/demodulator implemented with Method B.

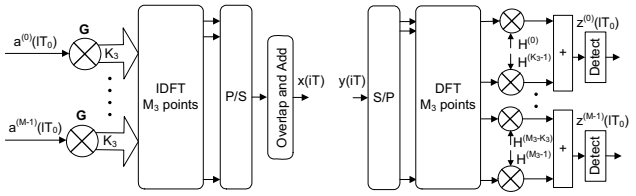

Fig. 4. FD implementation of the FMT system (Method C).

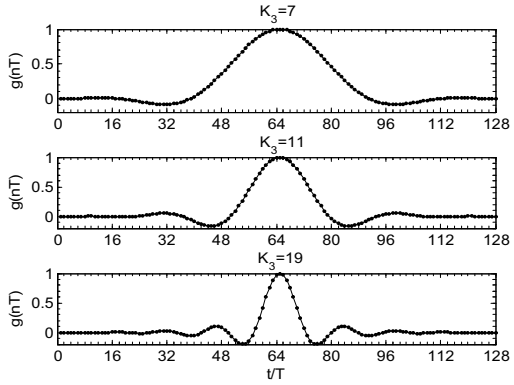

Fig. 5. Prototype pulse synthesized in the FD with K_3 frequency components.

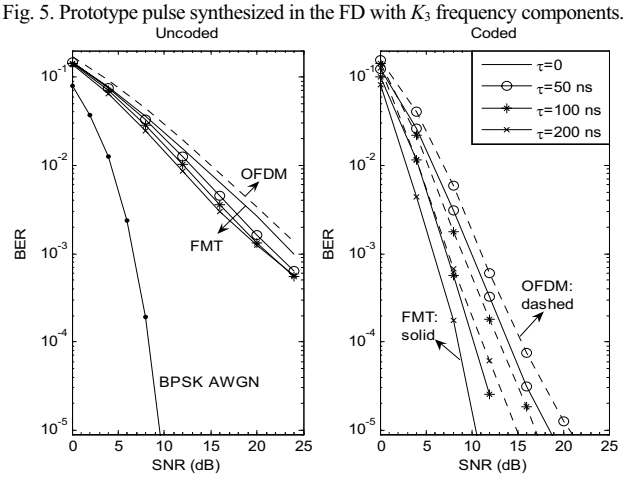

Fig. 6. Performance comparison between uncoded/coded FMT and OFDM.

REFERENCES

[1] Z. Wang, G. Giannakis, "Wireless multicarrier communications," *IEEE Signal Proc. Mag.*, pp. 29-48, May 2000.

[2] G. Cherubini, E. Eleftheriou, S. Ölçer, "Filtered multitone modulation for very high-speed digital subscribe lines," *IEEE JSAC*, pp. 1016-1028 , June 2002.

[3] N. Benvenuto, S. Tomasin, L. Tomba, "Equalization methods in DMT and FMT systems for broadband wireless communications," *IEEE Tr. on Comm.*, vol. 50, no. 9, pp. 1413-1418, Sept. 2002.

[4] A. Tonello, "Performance limits for filtered multitone modulation in fading channels," *IEEE Tr. Wireless Comm.*, pp. 2121, Sept. 2005.

[5] A. Tonello, "Asynchronous multicarrier multiple access: optimal and sub-optimal detection and decoding," *Bell Labs Technical Journal*, vol. 7, no. 3, pp. 191-217, 2003.